

PREDICTION OF ABNORMAL NEURAL CIRCUITS FOR DIAGNOSIS OF ALZHEIMER'S DISEASE

P. Dinesh Kumar

Department of Computer Science, Kodaikanal International School, India

Abstract

Alzheimer's disease (AD) is a neurological condition that causes memory loss and cognitive impairment and is gradual and irreversible. Timely intervention and a better quality of life for a patient are possible only through early and accurate diagnosis. This paper seeks to model abnormal neural circuits with brain networks that forecast a sound and timely detection of AD via cutting-edge neuroimaging methods. The Decoupling Generative Adversarial Network (DecGAN) is suggested to identify aberrant neural networks associated with AD. A decoupling module in the model separates brain networks into (i) a sparse network of the brain that contains circuits of great significance, and (ii) an additional network of trivial disease contribution. A conflicted learning scheme guarantees the emphasis on the features that are related to the disease, whereas a sparse capacity loss operation maintains the inherent topographical arrangement of neural networks. The model is trained and tested on DTI and rs-fMRI data of ADNI. Performance is evaluated using ROC-AUC, accuracy, precision, recall, F1-score, and training & validation loss. The proposed DecGAN had 92.1% accuracy, 89.2% precision, 86.5% recall, and 87.1% F1-score, with a ROC-AUC of 93.8% and a final validation loss of 0.0040 and it was significantly better than the current baseline and advanced classification methods. Superior discriminative performance for early-stage AD detection is indicated by a higher ROC-AUC, while better convergence, greater generalization, and less overfitting are demonstrated by lower validation loss. In this work, a sparse capacity loss function that maintains the neural circuit's topological distribution during decoupled graph reconstruction is introduced for the first time. Proposed methodology allows robust detection of AD-related aberrant circuits even under moderate changes in brain network structure by explicitly restricting sparsity and topology combined. Previous AD classification approaches based on GANs were unable to capture this capability.

Keywords:

Alzheimer's Disease, Generative Adversarial Network, Deep Learning (DL), Magnetic Resonance Images (MRI), Random Forest

1. INTRODUCTION

Alzheimer's disease (AD) accounts for 60–70% of all dementia cases and affects about 55 million people globally [1]. It is the most prevalent type of dementia. Patients' memory, cognition, and behavior gradually deteriorate as a result of this progressive and irreversible neurodegenerative disease, which is very expensive for patients, caregivers, and healthcare systems. Early and precise diagnosis is of the utmost essence since early treatment of the disease can slow the disease process and enhance quality of life [2]. Nevertheless, AD is a major clinical challenge to detect, particularly at its initial stages, like the Mild Cognitive Impairment (MCI) [3].

Neuroimaging techniques such as structural MRI, diffusion tensor imaging (DTI), and resting-state functional MRI (rs-fMRI) have surfaced as a potent instrument of AD diagnosis [4]. The modalities offer complementary knowledge of the anatomy and

physiology of the brain that enables us to create brain connections networks [5]. Specifically, DTI measures white matter integrity, whereas the functional interactions between the brain regions are measured by rs-fMRI [6]. Fig.1 shows that overall size of the gray matter in brain changes instantly from healthy individuals (CN) to MCI and eventually to AD, indicating the progression of the disease.

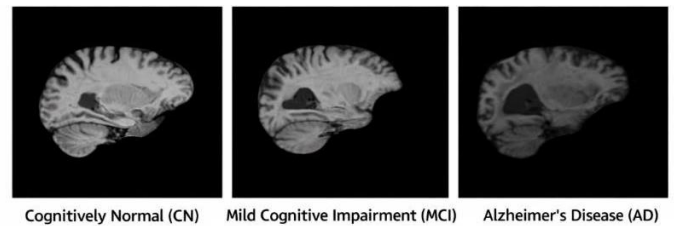


Fig.1. Progression of gray matter atrophy from CN to MCI and AD

In spite of their developments, it is still challenging to detect abnormal neural circuits of such complex brain networks because of their high dimensionality, noise, and complex topological structure [7]. Current methods of AD classification can be roughly divided into the traditional machine learning (ML) and deep learning (DL) methods [8]. Conventional methods use handcrafted characteristics and may not be able to detect any complex non-linear correlations within neuroimaging data. Despite being able to automatically extract features, DL models have several shortcomings: (i) lack of interpretability, (ii) are prone to overfitting, (iii) most often use single-modality data, and (iv) do not explicitly reveal disease-relevant neural connections and irrelevant ones [9], [10].

In addition, most of the currently implemented approaches do not consider the brain network as a single structure and instead do not retain its natural topology, compromising the ability to detect fine abnormalities. Generative models developed so far have mostly been used to address data augmentation, but not to explicitly find abnormal neural circuits [11], [12], [13]. These shortcomings demonstrate a major research gap: that a cohesive framework does not exist that can decouple brain networks into diagnostically useful and non-useful parts, maintain their topological properties, and that can detect abnormal neural networks with high confidence.

In order to resolve this, a Decoupling Generative Adversarial Network (DecGAN) is introduced in this work. The model suggested provides a decoupling mechanism separating brain networks into sparse neural circuit representations and additional parts with insignificant contributions to AD. Moreover, a new sparse capacity loss operation is created to maintain the natural topological distribution of brain circuits, which is robust to small changes in brain connectivity statistics. This allows for a better interpretation and detection of early-stage AD. The suggested

framework will be tested on the multimodal neuroimaging data (DTI and rs-fMRI) of the ADNI dataset.

The key contributions of the present work are the following:

- To suggest a new DecGAN structure that trains the brain networks in disease-relevant and noninformative parts, which allows the detection of abnormal circuits.
- To maintain the topological distribution of the neural circuits, a sparse capacity loss function is added to help enhance robustness and interpretability.
- To use a multimodal learning approach (DTI +rsfMRI) to obtain complementary structural and neural brain data.
- To show the superiority of the proposed DecGAN in terms of accuracy, precision, recall, F1-score, loss values, and ROC curve analysis by offering a thorough comparison against existing approaches.

This paper's remaining sections will be organized as follows:

A review of relevant work and limits will be carried out in Section 2. Section 3 provides an outline of the suggested methodology. Experimental results and a comparison are presented in Section 4. The paper is concluded in Section 5.

1.1 GENERATIVE ADVERSARIAL NETWORK (GAN)

GAN refers to a category of AI algorithms used in artistic development in an unsupervised ML model that employs two parts, especially generator and discriminator that use DL techniques to compete with one another [14]. The generator, being a convolutional neural network, tries to develop synthetic outputs that are similar to real data. A deconvolutional neural network acts as a discriminator in determining whether data is real or artificially generated by the generator. Throughout training, the discriminator got better at spotting false data, while the generator kept becoming better at creating realistic examples. This forms motivation between both networks for coming up with a well-formed output of high quality and realism, eventually by the generator.

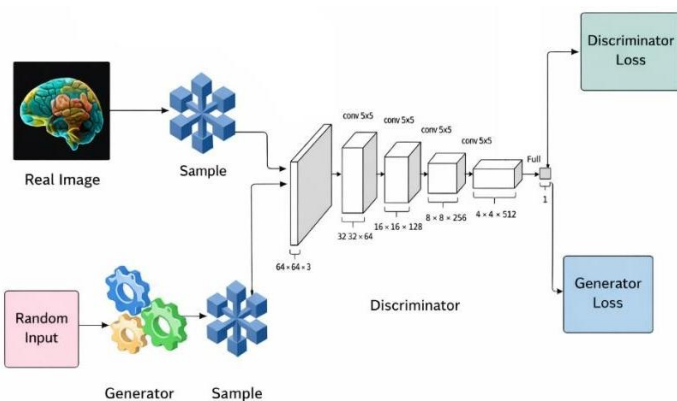


Fig.2. Architecture of GAN

GANs come in various types: Vanilla, Conditional, Deep convolutional, Cycle, Style, and Super resolution GAN. These are based on the three main principles: firstly, a generative model learns to generate data using a probabilistic notation. Secondly, training is performed in a conflicting situation where the generator competes against the discriminator. Lastly, GANs utilize deep

neural networks and artificial intelligence for training. GANs can be employed in unsupervised, supervised, and reinforcement learning settings.

The Fig.2 represents the architecture of GAN. When implementing GANs for generating 3D patterns of images, a random generator & discriminator are configured. The generator must comprehend the type of image; the Discriminator is trained on 2D image labeling with a label $y = 1$ for real images and $y = 0$ for generated 3D images. Discriminator calculates the image weights & provides feedback to the generator. This iterative process continues until the generator produces 3D image features effectively. The GAN framework has proven that it is powerful tool in various image generation and synthesis tasks across different domains [15]. This paper's main goal is to investigate this gap for AD detection. Using datasets of ADNI, the suggested DecGAN architecture makes use of explanatory power to comprehend AI decisions

2. RELATED WORKS

The use of ML and DL techniques in the diagnosis of AD has been extensively investigated in recent years. A general systematic review conducted by [16] analyzed more than 150 studies using DL as an AD detector, with the emphasis on the fact that CNN-based methods are prevalent in the literature, yet they do not explicitly model the topology of brain networks. Equally, [17] has thoroughly examined the DL approaches to predicting AD, which showed the absence of multimodal integration and preservation of topological features as the main research gaps.

Other groups have examined handwriting-based behavioral biomarkers of AD detection. [18] Also used 1D Convolutional Neural Networks to identify AD using online handwriting samples, showing encouraging outcomes with sequential behavioral cues, and [19] used semi-supervised learning to discover cognitive profiles using handwritings, whereas [20] used spatiotemporal dynamics of handwritings to characterize earlystage AD. Despite their novelty, these methods have restrictions due to the use of only one behavioral modality and cannot recap neuroimaging-derived structural and functional connectivity characteristics.

AD classification. Time-series GAN architectures have been used to overcome data scarcity. TimeGAN was proposed by [21] as a synthetic time-series generator, and [22] proposed a DoppelGANger as a networked time-series data generator. Although they enhance the availability of data, these methods do not solve the issue of neural circuit identification on the basis of the brain connectivity graph.

Direct methods of neuroimaging have been directed more specifically to brain network analysis. A multi-modal neuroimaging feature selection method with consistent metric constraint (MFCC) for AD analysis is proposed by [23], which used uniform metric constraints, but failed to maintain the neuralcircuit linkages and topological connectivity between ROIs. [24] created a hierarchical fully convolutional network (H-FCN) to localize atrophy using structural MRI but using only one modality. [25] developed a multi-scale enhanced graph convolutional network (MSE-GCN) for the identification of moderate cognitive impairment. This network used graph convolution to integrate structural and functional brain networks;

however, it was unable to differentiate between neural circuits connected to those unrelated to the condition.

Reliant on deep CNN models and ensemble learning to classify AD based on the brain MRI without using functional connectivity was achieved in [26]. [27] proposed an explainable ML model to classify AD based on the importance of features, but it is based on hand-constructed features and does not model complex nonlinear and circuit interactions. In order to diagnose AD, [28] suggested a group self-calibrated coordinate attention network (GSCANet) based on multimodal MRI. This network enhanced feature interaction through attention mechanisms, but it

was unable to explicitly characterize neural-circuit structure and connections across brain areas.

[29] suggested a framework of AI that predicts AD based on cortical features of T1-weighted MRI; however, it is restricted to structural data and lacks information about the functional connectivity. [30] proposes a prognostic model that uses functional connectome manifolds to predict AD conversion. While this model captures global functional connectivity patterns, it is unable to identify localized disease-related brain circuits and their topological relationships. The comparison of existing methods for AD detection is displayed in Table.1.

Table.1. Comparison of Existing AD Detection Approaches

Ref	Method / Type	Data/ Modality	Key Idea	Strength	Limitation
[16]	Review (DL-based)	Multiple	Survey of DL models for AD detection	Highlights the dominance of CNN methods	Does not address brain network topology
[17]	Review (DL-based)	Multi modal	Analysis of DL for AD prediction	Identifies research gaps	Lacks experimental validation
[18]	1D CNN	Hand writing	Uses sequential handwriting signals	Captures behavioural patterns	Limited to a single modality
[19]	Semi-supervised Learning	Hand writing	Learns cognitive profiles from handwriting	Reduces labelling effort	Ignores neuroimaging features
[20]	Spatiotemporal Analysis	Hand writing	Models dynamic handwriting patterns	Early stage detection potential	No brain connectivity modelling
[21]	GAN (TimeGAN)	Timeseries	Generates synthetic timeseries data	Addresses data scarcity	No neural circuit identification
[22]	GAN (DoppelGANger)	Timeseries	Generates realistic synthetic timeseries data	Improves data availability	Does not model brain connectivity or neural circuits
[23]	MFCC (Feature Selection method)	Multi modal Imaging	Selects discriminative imaging features	Improves classification	Ignores connection between brain regions and solely uses ROI data from MRI and PET
[24]	H-FCN	Structural MRI	Detects brain atrophy regions	Good spatial feature learning	Single modality only
[25]	MSE-GCN	Brain Networks	Multiscale graph learning for MCI detection	Captures connectivity patterns	Does not separate disease related and irrelevant neural circuits.
[26]	CNN + Ensemble	MRI	Combines deep CNN and ensemble learning	High classification accuracy	Ignores functional connectivity
[27]	Explainable ML	Imaging Features	Feature importance-based classification	Improves interpretability	Relies on handcrafted features
[28]	GSCANet	MRI (Multi modal)	Attention -based feature learning	Better feature representation	No explicit graph/circuit modelling
[29]	AI Model	T1weigh ted MRI	Uses cortical structural features	Strong structural prediction	Lacks functional connectivity
[30]	Connectome -based Prognostic Model	Functional MRI	Uses manifold learning on brain networks	Captures global connectivity	No localized circuit detection

2.1 RESEARCH GAPS

Despite significant progress in AD detection, there are still a number of important research gaps. Current techniques are mostly based on one mode of data or consider multimodal data separately, thus lacking the capability of modeling all interactions

within the brain. Most DL methods are trying to represent images without directly capturing brain connectivity, thus not discovering neural circuits that are interesting in disease. Graphbased techniques are partial in connectivity but do not offer any means to distinguish between meaningful and unimportant connections or maintain the topological structure of brain networks. Also,

explainable models typically rely on manually engineered features and are unable to model nonlinear relationships. Moreover, the vast majority of generative models are focused on data sparsity as opposed to circuit-level abnormality detection. The above limitations emphasize the necessity of a single framework that incorporates multimodal data, maintains topological characteristics, and clearly determines the abnormal neural networks to accurately and meaningfully diagnose the onset of an early-stage AD.

3. METHODOLOGY

In order to detect Alzheimer's disease, a Decoupling Generative Adversarial Network (DecGAN) method is put forth that divides brain connectivity networks into neural circuits that are diagnostically relevant and irrelevant while maintaining their topological connections. The suggested framework uses adversarial learning to further reconstruct these neural circuits to produce reliable and discriminative representations for precise AD classification.

3.1 DATASET

This study utilizes neuroimaging data from the Alzheimer's Disease Neuroimaging Initiative (ADNI) public dataset, which is available at <https://adni.loni.usc.edu>. The study focuses on four diagnostic stages of AD: Normal Control (NC), Early Mild Cognitive Impairment (EMCI), Late Mild Cognitive Impairment (LMCI), and AD. Multimodal neuroimaging data in NIfTI format, including DTI and rs-fMRI images, have been used for model validation and training. The study included 236 subjects, whose demographic details are presented in Table.2.

Table.2. Dataset

Group	AD	LMCI	EMCI	NC
Male (M)	34(M/62)28	22(M/42)20	38(M/55)17	33(M/74)42
Age	76.3±5.F	73.9±6.F	74.9±6.F	73.9±6.F

The rs-fMRI data were preprocessed using DPARSF and GREYNA toolboxes. DICOM format is converted to NIFTI for further analysis. DPARSF was used in standard preprocessing of fMRI data, which includes timing correction, motion correction, and spatial smoothing.

3.2 PRE-PROCESSING

Enhancing model performance for Alzheimer's disease detection relies on effectively preparing image data through preprocessing. The dataset is first standardized so that pixel values match from one photograph to another and so that biases caused by differences in illumination or imaging instruments are minimized. Median Filtering Process is one commonly used technique for noise suppression in digital image processing. This works by replacing each pixel with an updated value for the neighbourhood median. It is defined by a sliding window centered on the processed pixel. Mathematically, let $g(x,y)$ represent the filtered image and $f(x,y)$ represent the original image. The median screening procedure is represented by Eq.(1):

$$g(x,y) = \text{median}\{f(x+i, y+j) | (i,j) \in \{\text{neighbourhood}\}\} \quad (1)$$

Pixel coordinates being processed are denoted by (x,y) , and the neighbourhood corresponds generally to a rectangular or square window having predefined dimensions. The median function returns the middle value when the pixel intensities are arranged in ascending order.

3.3 FEATURE EXTRACTION

Detecting AD requires finding specific attributes in medical imaging that can differentiate healthy tissues from aberrant ones. The attributes may include shape, texture, intensity values, or spatial relationships within brain tissue. These features are used for classification to allow an accurate diagnosis and localization of putative anomalies. Variational Autoencoders (VAEs) form an important part of feature extraction in an unsupervised mode. In case of MRI scans for AD detection, VAE learns to encode input images (x) into latent vectors (z) in a way that stores the most important information in a form by Eq.(2):

$$z \sim q_\phi(z|x) = N(\mu_\phi(x), \sigma_\phi^2(x)) \quad (2)$$

where, q_ϕ represents the encoder, whereas the latent space distribution's mean and variance are represented by $\mu_\phi(x)$ and $\sigma_\phi^2(x)$, respectively.

3.4 PROPOSED DECGAN CLASSIFICATION FRAMEWORK

A novel method for detecting abnormal neural circuits associated with AD is the decoupling generative adversarial network (DecGAN) shown in Fig.3. A decoupling module that divides a brain network into two components is introduced by DecGAN. The first consists of sparse graphs representing neural circuits, which had a remarkable consequence on AD development. The second part includes an additional chart, the impact of which on AD can be disregarded.

To identify crucial neural circuits, the detected circuits are encoded into hypergraph data. The DecGAN generator reconstructs the brain network using the latent variable and the output from the decoupling module. After reconstructing, it is fed into the decoupling module to acquire sparse subgraphs $\{G_i\}$. Sparse capacity loss (L_{cap}) compares spatial-spectral differences between $\{G_i\}$ and $\{G_i\}$. Minimizing L_{cap} enhances the model's accuracy and robustness significantly. By employing this approach, researchers aim to improve the detection of abnormal neural circuits related to AD, contributing to a better understanding and potentially earlier diagnosis of the disease.

3.5 GCN DECOUPLING MODULE

The multimodal imaging data have been compiled for a comprehensive chart. Brain networks are derived from rs-fMRI and DTI analyses represented as an undirected weighted graph $G = (V, \mathcal{E})$, where sets of nodes and edges are denoted by V, \mathcal{E} , respectively. The architecture decoupling module is illustrated in Fig.4, in which layer identifies neural circuits by selecting optimal k nodes v_i .

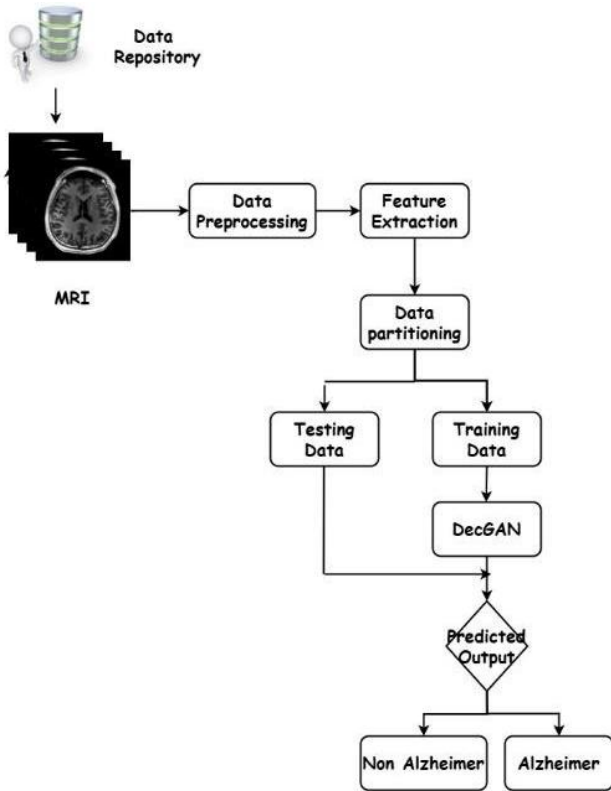


Fig.3. Architecture of Proposed DecGAN Framework

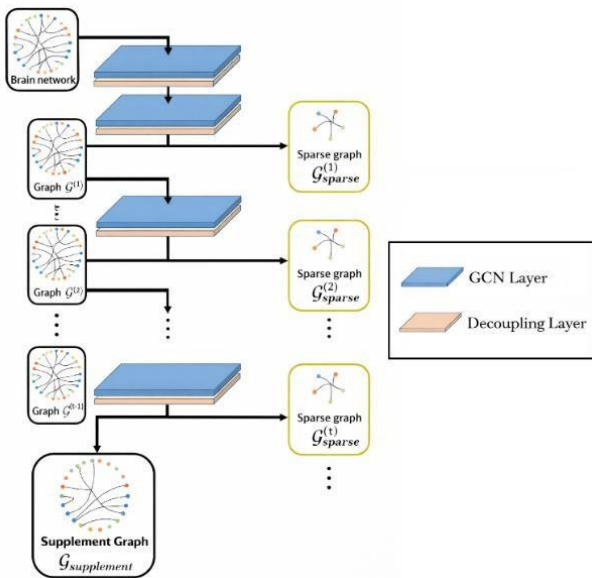


Fig.4. Architecture of the decoupling module

3.6 HYPERGRAPH AND ANALYTIC MODULE

Finding the brain pathways that affect AD is the decoupling module's primary objective. To ensure detected circuits are relevant, an analytic module was designed, using a hypergraph related algorithm. The notation for a hypergraph is $H=(V,\mathcal{E})$, where V and \mathcal{E} stand for the set of vertices and hyperedges that provide connections between several vertices. The framework of hypergraph H is represented by $|V|\times|\mathcal{E}|$ incidence matrix H ,

facilitating analysis of AD progression related to the identified neural circuits.

3.7 GENERATOR AND DISCRIMINATOR

Generator G performs reconstruction of the brain network using sparse graph $G_{sparse}^{(t)}$ and supplementary graph G_{supp} .

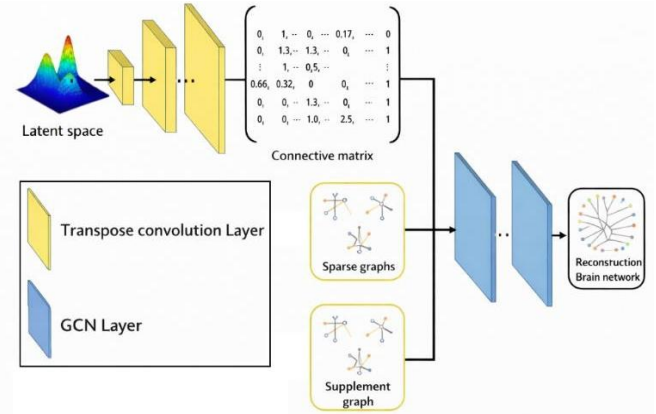


Fig.5. Structure of the generator

The Fig.5 illustrates the structure of both the generator and discriminator. The reconstruction process involves two steps. Firstly, the weighted adjacency matrix of the brain network is reconstructed and defined as $G(z, G_{sparse}^{(1)}, G_{sparse}^{(2)}, \dots, G_{sparse}^{(t)}, G_{supp})$.

Discriminator D is designed to differentiate between real and synthetic brain networks and comprises a Graph Convolutional Network (GCN) followed by a fully connected layer.

3.8 LOSS FUNCTIONS

The analytical loss is applied to optimize both the analytical and decoupling modules. The formula for analytical loss is denoted in Eq.(3), capturing the significance of detected neural circuits in AD progression.

$$L_{lanl} = E_G [-\log p_c(y|G_{sparse}^{(1)}, \dots, G_{sparse}^{(t)})] \quad (3)$$

It also ensures high accuracy while using the detected sparse graphs as inputs. Adversarial loss is used to train the Generator and Discriminator. The main goal is to construct a reconstructive similar brain network from the beginning of the brain network, which is defined in Eq.(4) and Eq.(5).

$$L_{Gadv} = E_{z,G} [\log D(G(z, G_{sparse}^{(1)}, \dots, G_{sparse}^{(t)}, G_{supp}))] \quad (4)$$

$$L_{Dadv} = E_G [\log D(G)] + E_{z,G} [\log(1 - D(G(z, G_{sparse}^{(1)}, \dots, G_{sparse}^{(t)}, G_{supp})))] \quad (5)$$

In the Sparse Capacity Loss, the decoupling module is improved based on feedback from the analytic module. It doesn't guarantee robust detection of neural circuits when the brain network's topological structure slightly changes. To address this, a novel sparse capacity loss L_{cap} is introduced, characterizing the structural difference between two sets of neural circuits (Eq.(6)). L_{cap} comprises of the spatial similarity $\text{sim}_{\text{spatial}}(H, H')$, spectral similarity $\text{sim}_{\text{spectral}}(H, H')$ of hypergraphs H and H' . This ensures

the decoupling module's robustness in detecting crucial neural circuits.

$$L_{cap} = \text{sim}_{\text{spatial}}(H, H') + \text{sim}_{\text{spectral}}(H, H') \quad (6)$$

3.9 RESULT AND DISCUSSION

Using the ADNI dataset, the suggested DecGAN approach is contrasted with current Alzheimer's disease detection techniques, which are Existing MFCC [23], H-FCN [24], MSE-GCN [25], GSCANet [28], and Prognostic Model [30]. Precision, F1-score, accuracy, recall, area under the curve (AUC), receiver operating characteristic (ROC), and training & validation loss are used to assess the performance of the suggested system.

- **Precision:** Measures the proportion of correctly predicted positives among all predicted positives using Eq.(7):

$$\text{Precision} = \frac{TP}{TP + FP} \quad (7)$$

- **Recall (Sensitivity):** It calculates the percentage of all actual positives that were accurately anticipated using Eq.(8):

$$\text{Recall} = \frac{TP}{TP + FN} \quad (8)$$

- **F1-Score:** Harmonic mean of recall and precision, balancing the two measurements through Eq.(9):

$$F1 = 2 \times \frac{\text{Precision} \times \text{Recall}}{\text{Precision} + \text{Recall}} \quad (9)$$

- **Accuracy:** Percentage of all samples that were accurately predicted through Eq.(10):

$$\text{Accuracy} = \frac{TP + TN}{TP + TN + FP + FN} \quad (10)$$

where, TP = True Positives, FP = False Positives, TN = True Negatives, and FN = False Negatives.

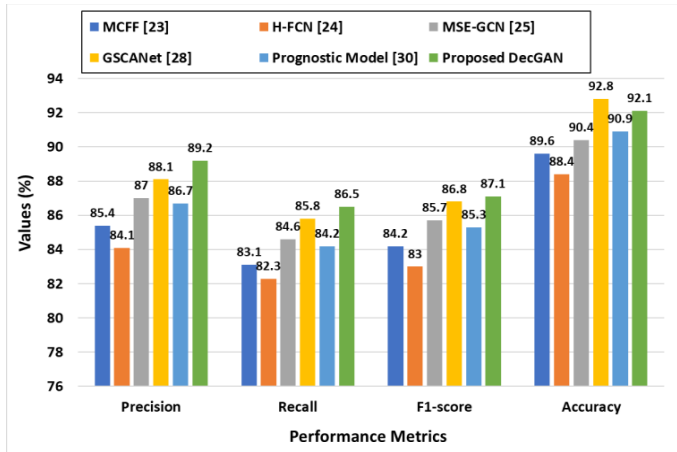


Fig.6. Comparison of Accuracy, Precision, Recall, and F1-Score

The Fig.6 shows that the suggested DecGAN framework outperforms existing AD detection techniques in terms of precision, recall, F1-score and accuracy. The adversarial feature generation in DecGAN can better preserve inter-regional neural interactions than the metric-constrained handmade features employed in MFCC, as seen by the proposed method's 2.5% improvement over the MFCC model's 89.6% accuracy. Because H-FCN only uses structural MRI, it is unable to fully capture the

complementary functional and topological information needed for early AD detection, resulting in an accuracy of only 88.4%, which is 4.2% lower than DecGAN. In a similar vein, MSE-GCN achieved 90.4% accuracy, whereas DecGAN gained an additional 1.7% by learning richer latent representations instead of relying just on random-walk embeddings and graph connections.

While the accuracy of GSCANet was slightly higher (92.8%) than DecGAN's (92.1%), its recall and F1-score were lower (85.8% and 86.8%, respectively) than those of the suggested approach (86.5% and 87.1%). This indicates that DecGAN is less likely to miss subtle early-stage AD cases and provides a more balanced categorization performance. The enhanced recall suggests that the adversarially produced latent representations are better at catching mild or ambiguous illness characteristics and lowering false negatives.

DecGAN also shows superior overall diagnostic performance as compared to the Prognostic Model, increasing accuracy, precision, recall, and F1-score by 2.5%, 1.6%, 1.3%, and 0.8%, respectively. The Prognostic Model's inferior discrimination performance for instant AD identification can be explained by the fact that it was primarily intended for long-term conversion-risk estimate using Cox regression and functional connectivity manifolds rather than direct classification. DecGAN, on the other hand, produces more precise and practically meaningful predictions by directly optimizing the illness classification job while maintaining multimodal neural-circuit information.

These results are in line with prior multimodal graph-based AD studies that shown that integrating structural and functional information enhances early AD detection and reported classification performance in the range of 89–94%. The improved discriminative capacity of the suggested DecGAN architecture is supported by recent interpretable graph-convolution and multimodal graph-learning techniques, which showed AUC values between 92% and 94%.

3.10 HYPERPARAMETER ANALYSIS

Two important factors were changed in a hyperparameter analysis to confirm the robustness of the suggested DecGAN framework: t and k . Here, t is the number of neural circuits recovered from the decoupling module, and k is the maximum number of selected areas of interest (ROIs). All other DecGAN training parameters, such as the dataset split, preprocessing method, optimizer, learning rate, batch size, and number of epochs, were held constant while the hyperparameter analysis was carried out on the binary AD versus NC classification task. In particular, t was varied among [1, 2, 3], while k was varied among [4, 5, 6, 7, 8]. The effects of different parameter combinations were evaluated using accuracy (ACC) and the area under the ROC curve (AUC). ACC measures the proportion of correctly categorized data, whereas AUC indicates the model's ability to distinguish AD patients from NC participants across all classification thresholds. AUC offers a more accurate indicator of clinical discrimination capacity since it is less impacted by threshold selection and class imbalance.

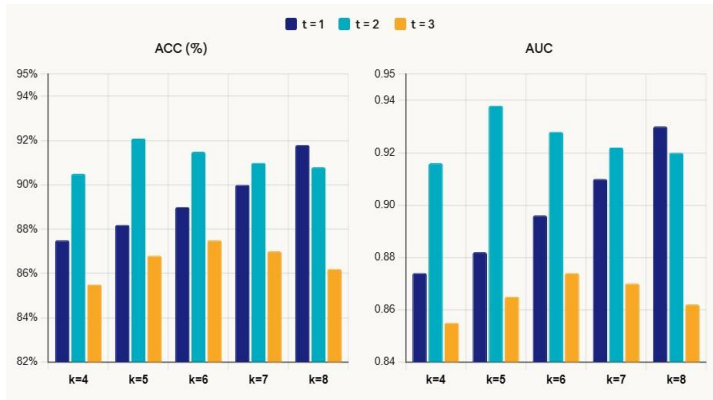


Fig.7. ACC, AUC comparison with various t, k

The ACC and AUC values obtained under various (t, k) combinations are shown in Fig.7. At $(t, k) = (2, 5)$, the suggested DecGAN gets the best ACC and AUC. The second-best performance is obtained at $(t, k) = (1, 8)$. The decoupling module isolates enough brain circuits to maintain complementary structural and functional relationships without adding unnecessary information when $t = 2$. In the same way, $k = 5$ offers an ideal number of discriminative ROIs, enabling the model to capture the most pertinent brain regions associated with Alzheimer's disease while avoiding noisy or unnecessary features. Conversely, higher values result in feature redundancy and mild overfitting, while lower values of t and k fail to reflect sufficient neuronal information.

Table.3. Hyperparameter Comparison with Existing Methods

Method	Hyper parameter	Tested Range/ Values	Optimal Setting	ACC (%)	AUC (%)
MFCC [23]	No. of selected handcrafted features	16,24,32,48	32 features	89.6	90.8
H-FCN [24]	No. of conv layers	2,3,4,5	4 layers	88.4	89.7
MSE-GCN [25]	Graph neighborhood size (k)	4,5,6,7,8	$k = 6$	90.4	91.5
GSCANet [28]	No. of graph-attention heads	2,4,8,12	8 heads	92.8	93.2
Prognostic Model [30]	No. of functional manifolds	3,5,7,9	5 manifolds	89.6	90.4
Proposed DecGAN	Neural circuit (t), ROI number (k)	$t = \{1,2,3\}$, $k = \{4,5,6,7,8\}$	$t=2$, $k=5$	92.1	93.8

The optimal hyperparameter settings of the suggested DecGAN are contrasted with current techniques in Table.3. The optimal performance of the suggested model is reached at $t=2$ and $k=5$, obtaining 92.1% ACC and 93.8% AUC. GSCANet has a lower AUC of 93.2% despite achieving a slightly higher ACC of 92.8%. As a result, DecGAN increases AUC by 0.6%, demonstrating its superior ability to differentiate between AD and NC individuals across various thresholds. AUC is regarded as a more accurate indicator for medical diagnosis since it is less impacted by threshold selection and class imbalance.

The findings corroborate earlier research demonstrating that achieving high performance requires careful hyperparameter selection. The best results are obtained with 32 handmade features for MFCC, four convolution layers for H-FCN, $k=6$ for MSEGNCN, and eight attention heads for GSCANet. These techniques are more susceptible to changes in the parameters, though. DecGAN, on the other hand, remains comparatively stable across different (t, k) combinations. The Fig.7 demonstrates that when $t=2$, raising k from 4 to 5 increases ACC from 90.5% to 92.1% and AUC from 91.6% to 93.8%; however, increasing k to 8 decreases ACC to 90.8% and AUC to 92.0%. This demonstrates how employing too many ROIs or neural circuits lowers performance and introduces redundant information.

The results also partially contradict previous research that, due to its higher ACC, thought GSCANet was the optimal approach. DecGAN has a better AUC and more balanced performance, which means it is more likely to identify cases of mild or ambiguous AD, even though GSCANet has the greatest ACC. Additionally, DecGAN outperforms MFCC, H-FCN, MSE-GCN, and the Prognostic Model, demonstrating that adversarial feature learning is superior to manually created features or traditional graph-based techniques. Therefore, the selected setting $(t=2, k=5)$ provides the best trade-off between accuracy, discrimination ability, and robustness, confirming the effectiveness and clinical reliability of the proposed DecGAN model. Recent evaluations of graph neural networks for AD diagnosis have found that multimodal graph models typically become less robust when too many connections or characteristics are included, which is consistent with the finding that moderate values of t and k offer the optimum results.

3.11 TRAINING AND VALIDATION LOSS

It gauges how well a model performs during training and evaluation; lower loss denotes better model performance, and tracking both training and validation loss aids in identifying overfitting or underfitting.

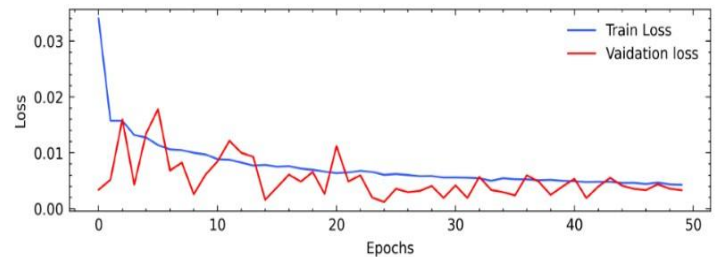


Fig.8. Training and Validation loss of the proposed DecGAN model

The Fig.8 displays the training and validation loss curves for the suggested DecGAN model across 50 epochs. Within the first ten epochs, the training loss drops dramatically from about 0.034 in the first epoch to about 0.010, suggesting that discriminative features are learned quickly. By epoch 50, it has steadily decreased and stabilized around 0.004. After that, it continuously declines with very slight fluctuations.

Table.4. Comparison of Training and Validation Loss with Existing Models Across Different Epochs

Epochs	Training Loss	Validation Loss					
	Proposed DecGAN	Proposed DecGAN	MFCC [23]	HFCN [24]	MSE-GCN [25]	GSCANet [28]	Prognostic Model [30]
10	0.010 2	0.011 8	0.02 05	0.01 86	0.01 69	0.0152	0.0224
20	0.007 1	0.008 3	0.01 64	0.01 48	0.01 26	0.0114	0.0185
30	0.005 6	0.005 4	0.01 37	0.01 15	0.00 97	0.0086	0.0153
40	0.004 8	0.004 6	0.01 19	0.00 98	0.00 81	0.0072	0.0132
50	0.004 1	0.004 0	0.01 05	0.00 87	0.00 70	0.0061	0.0118

Similar to this, the validation loss varies at first, peaking momentarily at roughly 0.018 in the early epochs as a result of adaptation to unseen data.

Both curves stabilize and stay quite close to one another after over 20 epochs; at the last epoch, they converge at 0.004. The convergence after about 30 epochs shows consistent and effective learning, furthermore, the small variance between the training & validation losses indicates that the proposed DecGAN model performs well in generalization with very little overfitting.

The Table.4 supports the effectiveness of the proposed DecGAN model by comparing its training and validation losses during different training epochs with those of previously published methods, such as MFCC, H-FCN, MSE-GCN, GSCANet, and the Prognostic Model. Every epoch, the suggested DecGAN consistently records the lowest validation loss, demonstrating quicker convergence and more robust generalization. Compared to MFCC (0.0205), H-FCN (0.0186), MSE-GCN (0.0169), GSCANet (0.0152), and the Prognostic Model (0.0224), DecGAN achieves a validation loss of 0.0118 at epoch 10. This translates to gains of 42.4%, 36.6%, 30.2%, 22.4%, and 47.3%, in that order. The suggested approach achieves a final validation loss of just 0.0040 by epoch 50, while MFCC, H-FCN, MSE-GCN, GSCANet, and the Prognostic Model maintain greater losses of 0.0105, 0.0087, 0.0070, 0.0061, and 0.0118, respectively. This pattern persists throughout training. DecGAN thus lowers the final validation loss by 61.9% when compared to MFCC, 54.0% when compared to H-FCN, 42.9% when compared to MSE-GCN, 34.4% when compared to GSCANet, and 66.1% when compared to the Prognostic Model.

These results corroborate previous research showing that deep graph-based and adversarial learning frameworks perform better for Alzheimer's disease identification than handmade and shallow-learning methods. The significant improvement over MFCC and the Prognostic Model demonstrates that Coxregression-based prognostic representations and manually created descriptors are inadequate to identify modest early Alzheimer related brain alterations. Similarly, DecGAN's superior performance over H-FCN and MSE-GCN suggests that adversarial acquired latent representations are more effective than purely CNN- or graph-based designs at preserving both multimodal and inter-regional neural information.

Additionally, because of its better classification accuracy, GSCANet, which was previously regarded as one of the best performing systems, is partially contradicted by the observed results. Despite achieving competitive predictive performance, GSCANet's validation loss is still greater than DecGAN's at

every epoch, particularly at epoch 50 (0.0061 against 0.0040). This implies that GSCANet has relatively poor generalization to unseen samples and is more likely to overfit. On the other hand, at epoch 50, the suggested DecGAN shows little change between its training loss (0.0041) and validation loss (0.0040), indicating consistent learning and little overfitting.

Recent multimodal AD frameworks that demonstrated sustained convergence and strong generalization when multimodal information was fused by graph-based learning are likewise compatible with the tight agreement between training loss and validation loss. The adversarial interaction between the discriminator and generator, which continuously improves latent features and increases the model's capacity to recognize mild and ambiguous AD patterns, is responsible for DecGAN's exceptional performance. As a result, Table.4 demonstrates that the suggested DecGAN offers more robust and clinically reliable early Alzheimer's disease diagnosis in addition to achieving lower loss and faster convergence than current techniques.

4. CONCLUSION

DecGAN, a novel Decoupling Generative Adversarial Network, is presented in this paper to identify aberrant neural networks in Alzheimer's disease. The proposed framework makes two key contributions: (i) a GCN-based decoupling module, which explicitly decouples the brain networks into diagnostically significant and sparse neural circuit graphs, and complementary non-AD-relevant components; and (ii) a new sparse capacity loss function (Lcap), which maintains the intrinsic graphical distribution of neural circuits during graph reconstruction and makes it resistant to changes in the brain network topology. This is, so far as we know, the first GAN-based AD detector that trains topological preservation of neural circuit distributions as an explicit training goal, which is a significant improvement over previous graph-based and GAN-based detectors.

Multimodal ADNI validation shows the state-of-the-art performance: 92.1% accuracy, 89.2% precision, 86.5% recall, and 87.1% F1-score, and better AUC using the 5-fold crossvalidation. These findings verify the top results of the DecGAN framework against five previous methods of both traditional ML and DL frameworks.

There are a number of weaknesses in the current research. To begin with, the ADNI dataset, although being highly popular, lacks the ability to reflect the demographic diversity of the actual AD population when it comes to age distribution, gender balance, and ethnicity, which may reduce the extent to which the trained

model could be generalised. Second, the specificity of models could be threatened, as, due to the similarity of structural alterations, the identification of the relevant AD biomarkers is complicated because such alterations may be found in other neurological disorders as well. Third, the existing architecture is based on a considerable portion of graph-level feature extraction; longitudinal neuroimaging data may also be incorporated to improve early detection accuracy.

The following future directions are suggested by this study: (i) validating the results on larger, demographically representative, and multisite datasets to increase the generalisability; (ii) combining other multimodal biomarkers (such as patterns of speech, dynamics in handwriting, EEG activity, etc.) with neuroimaging features; (iii) exploring transformer-based architectures and attention-based graph neural networks models in the framework of DecGAN; and (iv) investigating the clinical application of DecGAN as a neuroimaging decision-support system. These techniques have the potential to significantly improve early diagnosis and treatment of AD and other neurodegenerative disorders when they are further developed.

REFERENCES

- [1] R. Guan, X. Wen, Y. Liang, D. Xu, B. He and X. Feng, "Trends in Alzheimer's Disease Research based Upon Machine Learning Analysis of PubMed Abstracts", *International Journal of Biological Sciences*, Vol. 15, No. 10, pp. 2065-2074, 2019.
- [2] Y. Ying and J.Z. Wang, "Illuminating Neural Circuits in Alzheimer's Disease", *Neuroscience Bulletin*, Vol. 37, No. 8, pp. 1203-1217, 2021.
- [3] M. Mian, J. Tahiri, R. Eldin, M. Altabaa, U. Sehar and P.H. Reddy, "Overlooked Cases of Mild Cognitive Impairment: Implications to Early Alzheimer's Disease", *Ageing Research Reviews*, Vol. 98, pp. 1-17, 2024.
- [4] R.A. Hazarika, A.K. Maji, S.N. Sur, B.S. Paul and D. Kandar, "A Survey on Classification Algorithms of Brain Images in Alzheimer's Disease based on Feature Extraction Techniques", *IEEE Access*, Vol. 9, pp. 58503-58536, 2021.
- [5] Z. Kong, J. Luo and S. Xu, "Automatic Tissue Image Segmentation based on Image Processing and Deep Learning", *Journal of Healthcare Engineering*, Vol. 2019, No. 1, pp. 1-10, 2019.
- [6] G. Awate, S. Bangare, G. Pradeepini and S. Patil, "Detection of Alzheimers Disease from MRI using Convolutional Neural Network with Tensorflow", *Proceedings of International Conference on Computer Vision and Pattern Recognition*, Vol. 29, pp. 1-10, 2018.
- [7] R. Biswas, D. Purkayastha and S. Roy, "Denoising of MRI Images using Curvelet Transform", *Advances in Systems, Control and Automation*, Vol. 442, pp. 575-583, 2017.
- [8] I. Ullah, M. Hussain, E.U.H. Qazi and H. Aboalsamh, "An Automated System for Epilepsy Detection using EEG Brain Signals based on Deep Learning Approach", *Expert Systems with Applications*, Vol. 107, pp. 61-71, 2018.
- [9] O. Yildirim, P. Pławiak, R.S. Tan and U.R. Acharya, "Arrhythmia Detection using Deep Convolutional Neural Network with Long Duration ECG Signals", *Computers in Biology and Medicine*, Vol. 102, pp. 411-420, 2018.
- [10] C. Taleb, L. Likforman-Sulem, C. Mokbel and M. Khachab, "Detection of Parkinson's Disease from Handwriting using Deep Learning: A Comparative Study", *Evolutionary Intelligence*, Vol. 16, pp. 1813-1824, 2023.
- [11] J. Pan, Q. Zuo, B. Wang, C.L.P. Chen, B. Lei and S. Wang, "DecGAN: Decoupling Generative Adversarial Network for Detecting Abnormal Neural Circuits in Alzheimer's Disease", *IEEE Transactions on Artificial Intelligence*, Vol. 5, No. 10, pp. 5050-5063, 2024.
- [12] X. Yi, E. Walia and P. Babyn, "Generative Adversarial Network in Medical Imaging: A Review", *Medical Image Analysis*, Vol. 58, pp. 1-17, 2019.
- [13] Y. Dong, W. Sawin and Y. Bengio, "HNHN: Hypergraph Networks with Hyperedge Neurons", *Proceedings of International Conference on Machine Learning*, Vol. 22, pp. 1-11, 2020.
- [14] Y. Skandarani, P.M. Jodoin and A. Lalande, "GANs for Medical Image Synthesis: An Empirical Study", *Journal of Imaging*, Vol. 9, No. 3, pp. 1-16, 2023.
- [15] S. Sabnam and S. Rajagopal, "Application of Generative Adversarial Networks in Image, Face Reconstruction and Medical Imaging: Challenges and the Current Progress", *Computer Methods in Biomechanics and Biomedical Engineering: Imaging and Visualization*, Vol. 12, No. 1, pp. 1-20, 2024.
- [16] E.M. Mohammed, A.M. Fakhrudeen and O.Y. Alani, "Detection of Alzheimer's Disease using Deep Learning Models: A Systematic Literature Review", *Informatics in Medicine Unlocked*, Vol. 50, pp. 1-34, 2024.
- [17] I. Malik, A. Iqbal, Y.H. Gu, M.A. Al-Antari, "Deep Learning for Alzheimer's Disease Prediction: A Comprehensive Review", *Diagnostics*, Vol. 14, No. 12, pp. 1-23, 2024.
- [18] Q. Dao, M.A. El-Yacoubi and A.S. Rigaud, "Detection of Alzheimer Disease on Online Handwriting using 1D Convolutional Neural Network", *IEEE Access*, Vol. 11, pp. 2148-2155, 2023.
- [19] M.A. El-Yacoubi, S. Garcia-Salicetti, C. Kahindo, A.S. Rigaud and V. Cristancho-Lacroix, "From Aging to Early-Stage Alzheimer's: Uncovering Handwriting Multimodal Behaviors by Semi-Supervised Learning and Sequential Representation Learning", *Pattern Recognition*, Vol. 86, pp. 112-133, 2019.
- [20] C. Kahindo, M.A. El-Yacoubi, S. Garcia-Salicetti, A.S. Rigaud and V. Cristancho-Lacroix, "Characterizing Early-Stage Alzheimer through Spatiotemporal Dynamics of Handwriting", *IEEE Signal Processing Letters*, Vol. 8, pp. 1136-1140, 2018.
- [21] J. Yoon, D. Jarrett and M. Van Der Schaar, "Time-Series Generative Adversarial Networks", *Advances in Neural Information Processing Systems*, Vol. 32, pp. 1-11, 2019.
- [22] Z. Lin, A. Jain, C. Wang, G. Fanti and V. Sekar, "Using GANs for Sharing Networked Time Series Data: Challenges, Initial Promise, and Open Questions", *Proceedings of International Conference on Internet Measurement*, Vol. 78, pp. 464-483, 2020.
- [23] X. Hao, Y. Bao, Y. Guo, M. Yu, D. Zhang and S.L. Risacher, "Multi-Modal Neuroimaging Feature Selection with Consistent Metric Constraint for Diagnosis of Alzheimer's Disease", *Medical Image Analysis*, Vol. 60, pp. 1-10, 2020.

- [24] C. Lian, M. Liu, J. Zhang and D. Shen, "Hierarchical Fully Convolutional Network for Joint Atrophy Localisation and Alzheimer's Disease Diagnosis using Structural MRI", *IEEE Transactions on Pattern Analysis and Machine Intelligence*, Vol. 42, No. 4, pp. 880-893, 2018.
- [25] B. Lei, Y. Zhu, S. Yu, H. Hu, Y. Xu, G. Yue, T. Wang, C. Zhao, S. Chen, P. Yang, X. Song, X. Xiao and S. Wang, "Multi-Scale Enhanced Graph Convolutional Network for Mild Cognitive Impairment Detection", *Pattern Recognition*, Vol. 134, pp. 1-9, 2023.
- [26] J. Islam and Y. Zhang, "Brain MRI Analysis for Alzheimer's Disease Diagnosis using an Ensemble System of Deep Convolutional Neural Networks", *Brain Informatics*, Vol. 5, No. 2, pp. 1-14, 2018.
- [27] A.S. Alatrany, W. Khan, A. Hussain, J. Shang and J. Zhang, "An Explainable Machine Learning Approach for Alzheimer's Disease Classification", *Scientific Reports*, Vol. 14, pp. 1-18, 2024.
- [28] X. Yu, J. Liu and Y. Lu, "Early Diagnosis of Alzheimer's Disease using a Group Self-Calibrated Coordinate Attention Network based on Multimodal MRI", *Scientific Reports*, Vol. 14, pp. 1-18, 2024.
- [29] R. Zeng, B. Yang, F. Wu, H. Liu, X. Wu and L. Tang, "Early Prediction of Alzheimer's Disease using Artificial Intelligence and Cortical Features on T1WI Sequences", *Frontiers in Neurology*, Vol. 16, pp. 1-15, 2025.
- [30] S. Kim, M. Kim, J.E. Lee, B.Y. Park and H. Park, "Prognostic Model for Predicting Alzheimer's Disease Conversion using Functional Connectome Manifolds", *Alzheimer's Research and Therapy*, Vol. 16, No. 1, pp. 1-11, 2024.